Dynamics of shape-invariant rotating beams in linear media with harmonic potentials

Juan Chen, Fushun Zhang, Kai Bian, Chaojie Jiang, Wei Hu, and Daquan Lu*

Guangdong Provincial Key Laboratory of Nanophotonic Functional Materials and Devices, South China Normal University, Guangzhou 510631, China

(Received 14 July 2018; published 5 March 2019)

We introduce a type of shape-invariant rotating beam in linear media with harmonic potentials. This type of beam is constructed by superposing a series of properly selected Laguerre-Gaussian beams of different orders. During propagation, the beam is shape invariant, but the pattern rotates and its size varies periodically. The transverse position of the beam at the exit plane of a medium can be steered by tuning the input parameters, even if the transverse position at the entrance plane is fixed.

DOI: 10.1103/PhysRevA.99.033808

I. INTRODUCTION

The manipulation of light beams is an important subject in the region of light transmission optics. In recent years, the external potentials, such as linear potentials and harmonic potentials, have been introduced as effective tools to manipulate beams. In linear potentials, it has been found that the propagation direction of Airy beams can be changed while preserving their nondiffracting properties [1,2], multicolor plasmonic Airy beams can be routed into different directions [3], the autofocusing points and strength can be steered [4–6], and an Airy beam can even propagate in any predefined path [7]. As for harmonic potentials, researchers have made in-depth investigation on various types of beams, such as Airy-Gaussian beams, hypergeometric beams, and beams carrying orbital angular momentum [8–17]. Some interesting effects, such as the periodic focusing [18], the designable self-Fourier beams [19], the periodic inversion [9,10], the phase transition [8,9], and the anharmonic oscillation [8,9,20], have been revealed. Besides, researchers have investigated the propagation dynamics of beams or pulses in other types of potentials, such as localized potentials [21], smooth-interface sigmoid-type potentials [21], and higher-order power-law potentials [22]. Some unique behaviors, such as the adjustable trajectory [21] and the revival or antirevival effects [22], have been discovered.

In this work, we report a type of combined beam, which is constructed by superposing a series of Laguerre-Gaussian (LG) beams of different orders, in linear media with harmonic potentials. If the constituent beams are properly selected, the combined beam keeps shape invariant and rotating during propagation. Beyond studying the rotation, we also go a step further to take into account the initial kick on the beam and the initial transverse displacement of the beam from the potential center, which together influence the transverse position of the beam at the exit plane of a medium with fixed length.

The rest of this paper is organized as follows: In Sec. II, by using the technique of variable transformation, we get the analytical solution of the shape-invariant rotating beam in a harmonic potential. In Sec. III, based on the analytical solution, we investigate the propagation dynamics of this type of beam. We conclude in Sec. IV.

II. MODEL

We consider beams in a linear medium with an external harmonic potential. In this case, the paraxial propagation of a beam is governed by the linear $(2+1)D$ Schrödinger equation [8,13]

$$2ik\frac{\partial \Psi}{\partial z}+\frac{\partial^2 \Psi}{\partial x^2}+\frac{\partial^2 \Psi}{\partial y^2}-k^2\alpha^2 r^2\Psi=0, \tag{1}$$

where $\Psi(x, y, z)$ is the complex envelop of the optical field, k is the wave number, and α determines the width of the external harmonic potential, which can be easily achieved, for example, in gradient-index media.

We construct the shape-invariant rotating beam by superposing a series of properly selected LG beams of different orders. The input field is

$$\begin{aligned}\Psi(\mathbf{r},0) &= \sum_{p,l} b_{p,l}\Psi_{p,l}(\mathbf{r},0)\\ &= \sum_{p,l} b_{p,l}\exp\left(-\frac{|\mathbf{r}-\mathbf{r}_0|^2}{2w_0^2}\right)\left(\frac{|\mathbf{r}-\mathbf{r}_0|}{w_0}\right)^{|l|}\\ &\quad\times L_p^{|l|}\left(\frac{|\mathbf{r}-\mathbf{r}_0|^2}{w_0^2}\right)\exp[il\varphi(0)]\exp(i\mathbf{C}_0\cdot\mathbf{r}),\end{aligned} \tag{2}$$

where $b_{p,l}$ are weight coefficients, $\mathbf{r}=(x,y)$ represents the two-dimensional (2D) transverse coordinate vector, w_0 is the beamwidth at $z=0$, $L_p^{|l|}(\cdot)$ is the generalized Laguerre polynomial, $p=0,1,2,\dots,$ $|l|=0,1,2,\dots,$ $\mathbf{C}_0=(C_{0x},C_{0y})$ represents the initial kick on the beam to move it in the transverse direction, $\mathbf{r}_0=(r_{0x},r_{0y})$ is the initial transverse displacement of the beam from the potential center, $\varphi(0)$ is the azimuthal angle around the beam center $\mathbf{r}=\mathbf{r}_0$. As will be shown in Sec. III, the combined beam can be kept shape invariant and rotating if the constituent LG beams are properly selected.

It is not easy to solve Eq. (1) directly. Fortunately, in our previous work [23] we have established a relationship between Eq. (1) and the paraxial propagation equation for

*ludq@scnu.edu.cn

beams in free space, i.e.,

$$2ik\frac{\partial \phi}{\partial z_f}+\frac{\partial^2 \phi}{\partial x_f^2}+\frac{\partial^2 \phi}{\partial y_f^2}=0. \quad (3)$$

Therefore, if its counterpart in free space [i.e., $\phi(\mathbf{r}_f, z_f)$, where $\mathbf{r}_f=(x_f, y_f)$] is known, the solution of Eq. (1) can be obtained based on the one-to-one correspondence [23]

$$\Psi(\mathbf{r}, z)=F_1F_2\times\phi(F_1\mathbf{r}, F_3), \quad (4)$$

where

$$F_1(z)=(-1)^a\left[1+\tan^2\left(\frac{z}{z_{c0}}\right)\right]^{1/2}, \quad (5)$$

$$F_2(\mathbf{r}, z)=\exp\left\{-\frac{ikF_1(z)^2r^2}{2z_{c0}\left[\tan\left(\frac{z}{z_{c0}}\right)+1/\tan\left(\frac{z}{z_{c0}}\right)\right]}\right\}, \quad (6)$$

$$F_3(z)=z_{c0}\tan\left(\frac{z}{z_{c0}}\right), \quad (7)$$

$$a(z)=\frac{1}{\pi}\left\{\frac{z}{z_{c0}}-\arctan\left[\tan\left(\frac{z}{z_{c0}}\right)\right]\right\}, \quad (8)$$

$$z_{c0}=kw_c^2, \quad w_c=\frac{1}{\sqrt{k\alpha}}. \quad (9)$$

Now the question becomes solving Eq. (3) to get the solution in free space for the input field,

$$\phi(\mathbf{r}_f, 0)=\sum_{p,l}b_{p,l}\exp\left(-\frac{|\mathbf{r}_f-\mathbf{r}_0|^2}{2w_0^2}\right)\left(\frac{|\mathbf{r}_f-\mathbf{r}_0|}{w_0}\right)^{|l|}\times L_p^{|l|}\left(\frac{|\mathbf{r}_f-\mathbf{r}_0|^2}{w_0^2}\right)\exp[il\varphi_f(0)]\exp(i\mathbf{C}_0\cdot\mathbf{r}_f), \quad (10)$$

where $\mathbf{r}_f=(x_f, y_f)$, $\varphi_f(0)$ is the azimuthal angle around the beam center $\mathbf{r}_f=\mathbf{r}_0$.

Because of the mathematical complexity induced by the initial kick $\mathbf{C}_0$ and the initial displacement $\mathbf{r}_0$, it is still not easy to directly get the solution of Eq. (3) for the input field shown in Eq. (10). However, we note that, if we introduce a set of transformation relations

$$\mathbf{r}'_f=\mathbf{r}_f-\mathbf{r}_0-\frac{\mathbf{C}_0}{k}z_f, \quad z'_f=z_f$$

and the variable transformation

$$\phi(\mathbf{r}_f, z_f)=\psi(\mathbf{r}'_f, z'_f)\exp\left(i\mathbf{C}_0\cdot\mathbf{r}_f-\frac{iC_0^2}{2k}z_f\right), \quad (11)$$

Eq. (3) becomes

$$2ik\frac{\partial \psi}{\partial z'_f}+\frac{\partial^2 \psi}{\partial x'^2_f}+\frac{\partial^2 \psi}{\partial y'^2_f}=0, \quad (12)$$

which in form is identical to Eq. (3). However, in the reference frame $(\mathbf{r}'_f, z'_f)$, the input field becomes

$$\psi(\mathbf{r}'_f, 0)=\sum_{p,l}b_{p,l}\exp\left(-\frac{r'^2_f}{2w_0^2}\right)\left(\frac{r'_f}{w_0}\right)^{|l|}\times L_p^{|l|}\left(\frac{r'^2_f}{w_0^2}\right)\exp[il\varphi'_f(0)], \quad (13)$$

where $\mathbf{r}'_f=(x'_f, y'_f)$, $\varphi'_f(0)$ is the azimuthal angle around the beam center $\mathbf{r}'_f=0$.

As shown in Eq. (13), in the reference frame $(\mathbf{r}'_f, z'_f)$, the input field is no longer with the initial kick and transverse displacement. Under this condition, we can easily obtain the solution of Eq. (12), which is the coaxial superposition of LG beams of different orders [24],

$$\psi(\mathbf{r}'_f, z'_f)=\frac{w_0}{w(z'_f)}\exp\left[-\frac{r'^2_f}{2w^2(z'_f)}\right]\exp\left[\frac{ikr'^2_f}{2R(z'_f)}\right]\sum_{p,l}b_{p,l}\left[\frac{r'_f}{w(z'_f)}\right]^{|l|}\times L_p^{|l|}\left[\frac{r'^2_f}{w^2(z'_f)}\right]\exp\left[-i(2p+|l|+1)\arctan\left(\frac{z'_f}{z_0}\right)\right]\exp[il\varphi'_f(z'_f)], \quad (14)$$

where $w(z'_f)=w_0[1+(z'_f/z_0)^2]^{1/2}$, $R(z'_f)=z'_f[1+(z_0/z'_f)^2]$, $z_0=kw_0^2$.

Based on Eqs. (14), (11), and (4), we finally obtain the exact analytical solution of Eq. (1) as

$$\Psi(\mathbf{r}, z)=\sum_{p,l}u_{p,l}(\mathbf{r}, z)\exp\left[i\mathbf{q}(z)\cdot\mathbf{r}+i\nu(z)+\frac{ik|\mathbf{r}-\mathbf{s}(z)|^2}{2R(z)}\right]\exp[il\varphi(z)+i\delta_{p,l}(z)], \quad (15)$$

where

$$u_{p,l}(\mathbf{r}, z)=b_{p,l}\frac{w_0}{w(z)}\exp\left[-\frac{|\mathbf{r}-\mathbf{s}(z)|^2}{2w^2(z)}\right]\left[\frac{|\mathbf{r}-\mathbf{s}(z)|}{w(z)}\right]^{|l|}\times L_p^{|l|}\left[\frac{|\mathbf{r}-\mathbf{s}(z)|^2}{w^2(z)}\right], \quad (16)$$

$$w(z)=w_0\left[1+\frac{w_c^4-w_0^4}{w_0^4}\sin^2\left(\frac{z}{z_{c0}}\right)\right]^{1/2}, \quad (17)$$

$$R(z)=\frac{1}{1+\tan^2\left(\frac{z}{z_{c0}}\right)}\frac{z_{c0}\tan\left(\frac{z}{z_{c0}}\right)}{\frac{1}{1+1/\left[\frac{z_{c0}}{z_0}\tan\left(\frac{z}{z_{c0}}\right)\right]^2}-\frac{1}{\left[1+1/\tan^2\left(\frac{z}{z_{c0}}\right)\right]}}, \quad (18)$$

$$\delta_{p,l}(z)=-(2p+|l|+1)\left\{a\pi+\arctan\left[\frac{w_c^2}{w_0^2}\tan\left(\frac{z}{z_{c0}}\right)\right]\right\}, \quad (19)$$

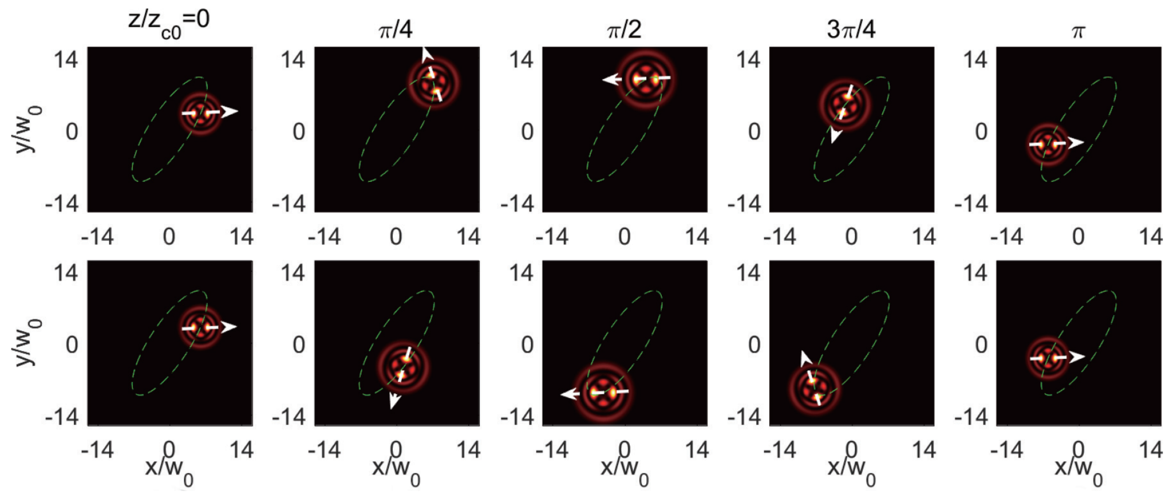

FIG. 1. Evolution of the shape-invariant rotating beam for different input conditions. Upper row: $C_{0x} = 3/w_0$, $C_{0y} = 7/w_0$, $\Psi(\mathbf{r}, 0) = 2\Psi_{0,1}(\mathbf{r}, 0) + 0.3\Psi_{1,3}(\mathbf{r}, 0) + 0.1\Psi_{2,5}(\mathbf{r}, 0)$. Bottom row: $C_{0x} = -3/w_0$, $C_{0y} = -7/w_0$, $\Psi(\mathbf{r}, 0) = 2\Psi_{0,-1}(\mathbf{r}, 0) + 0.3\Psi_{1,-3}(\mathbf{r}, 0) + 0.1\Psi_{2,-5}(\mathbf{r}, 0)$. The values of the other parameters are $r_{0x} = 6w_0$, $r_{0y} = 3w_0$, $w_0/w_c = 0.85$.

$$\mathbf{s}(z) = \frac{1}{(-1)^a\left[1+\tan^2\left(\frac{z}{z_{c0}}\right)\right]^{1/2}}\left[\mathbf{r}_0 + \frac{\mathbf{C}_0}{k} z_{c0}\tan\left(\frac{z}{z_{c0}}\right)\right], \tag{20}$$

$$\mathbf{q}(z) = \frac{1}{(-1)^a\left[1+\tan^2\left(\frac{z}{z_{c0}}\right)\right]^{1/2}}\left[\mathbf{C}_0 - k\frac{\mathbf{r}_0}{z_{c0}}\tan\left(\frac{z}{z_{c0}}\right)\right], \tag{21}$$

$$\nu(z) = \mathbf{C}_0\cdot\mathbf{r}_0\sin^2\left(\frac{z}{z_{c0}}\right) + \frac{k}{4}\left[\frac{\mathbf{r}_0^2}{z_{c0}} - z_{c0}\left(\frac{\mathbf{C}_0}{k}\right)^2\right]\sin\left(\frac{2z}{z_{c0}}\right); \tag{22}$$

$\varphi(z)$ is the azimuthal angle around the beam center $\mathbf{r} = \mathbf{s}(z)$, which varies during propagation.

Equation (15) is the main result, which describes the propagation of the shape-invariant rotating beam in a linear medium with an external harmonic potential. We will discuss the propagation dynamics in the next section.

III. PROPAGATION DYNAMICS

Based on the analytical solution, i.e., Eq. (15), we can study the propagation dynamics of the shape-invariant rotating beam in this section. Figure 1 shows the general propagation properties: the pattern shape is invariant but its size changes periodically; the pattern rotates clockwise or anticlockwise around the beam center; and the transverse position of the beam continuously changes in the transverse plane. Below we will discuss these properties in detail.

A. Prerequisite of the shape-invariant rotation

The rotation of the beam can be explained in the view of the relation between the phase vortex and the Gouy phase shift of each constituent beam. As shown in Eq. (19), during propagation each constituent beam experiences its own Gouy phase shift, i.e., $\delta_{p,l}(z)$. Therefore, the intensity distribution of the combined beam can be written as

$$\begin{aligned}|\Psi|^2 &= \left|\sum_{p,l} u_{p,l}(r,z)\exp[il\varphi(z) + i\delta_{p,l}(z)]\right|^2 \\ &= \left|\sum_{p,l} u_{p,l}(r,z)\exp\{il[\varphi(z)-\varphi_0(z)] + i\chi(z)\}\right|^2 \\ &= \left|\sum_{p,l} u_{p,l}(r,z)\exp\{il[\varphi(z)-\varphi_0(z)]\}\right|^2,\end{aligned} \tag{23}$$

where

$$\varphi_0(z) = \frac{2p+|l|+\beta}{l}\left\{a\pi + \arctan\left[\frac{w_c^2}{w_0^2}\tan\left(\frac{z}{z_{c0}}\right)\right]\right\}, \tag{24}$$

$$\chi(z) = (\beta-1)\left\{a\pi + \arctan\left[\frac{w_c^2}{w_0^2}\tan\left(\frac{z}{z_{c0}}\right)\right]\right\}; \tag{25}$$

β is an arbitrary real number. We note that when the prerequisite

$$\begin{cases}\frac{2p+|l|+\beta}{l} = \text{const} & (\text{for } \beta \neq 0)\\ \frac{2p+|l|+\beta}{l} = \text{const} \vee p = l = 0 & (\text{for } \beta = 0)\end{cases} \tag{26}$$

is satisfied, the phase vortex of each constituent beam at $z = z$ is rotated by the same angle $\varphi_0(z)$, which increases monotonically with the propagation distance z. Subsequently, the pattern of the combined beam, which is induced by the coherent superposition of the constituent beams, is shape invariant but rotates in synchronization with the phase vortex during propagation. As shown in Eqs. (23) and (24), the pattern rotates clockwise (anticlockwise) when the topological charges $l < 0$ ($l > 0$).

In the special case that

$$\frac{p}{l} = 1, \tag{27}$$

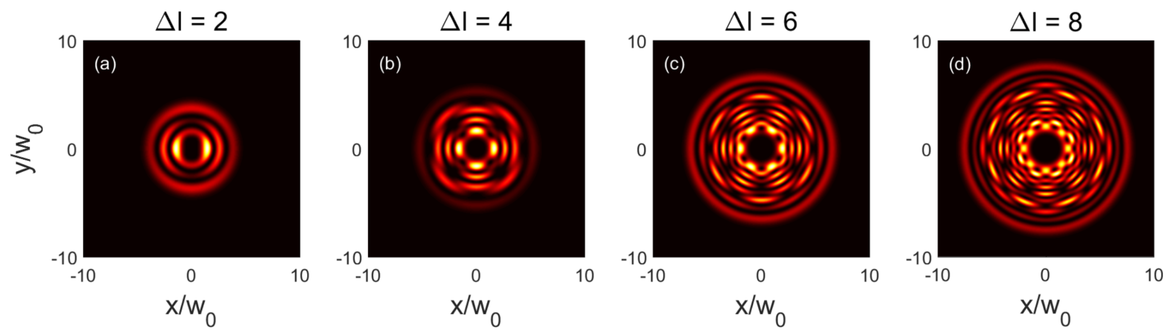

FIG. 2. Some examples of the intensity pattern of the rotating beam at the entrance plane for different Δl, which is the minimum interval of the topological charges for the constituent beams. (a) $\Psi(\mathbf{r},0)=\Psi_{0,1}(\mathbf{r},0)+\Psi_{1,3}(\mathbf{r},0)+0.3\Psi_{2,5}(\mathbf{r},0)$, (b) $\Psi(\mathbf{r},0)=10\Psi_{0,1}(\mathbf{r},0)+40\Psi_{2,5}(\mathbf{r},0)+0.1\Psi_{4,9}(\mathbf{r},0)$, (c) $\Psi(\mathbf{r},0)=10\Psi_{0,1}(\mathbf{r},0)+100\Psi_{3,7}(\mathbf{r},0)+0.01\Psi_{6,13}(\mathbf{r},0)$, (d) $\Psi(\mathbf{r},0)=30\Psi_{0,1}(\mathbf{r},0)+900\Psi_{4,9}(\mathbf{r},0)+0.001\Psi_{8,17}(\mathbf{r},0)$.

the intensity distribution of the shape-invariant rotating beam becomes

$$|\Psi|^2=\left|\sum_n u_{n,n}(\mathbf{r},z)\exp\{in[\varphi(z)-\varphi_0(z)]\}\right|^2, \tag{28}$$

which is the superposition of the LG beams with the minimum interval of the indices, i.e., $\Delta p=\Delta l=1$, where $n=p=l=0,1,2\ldots$. In Ref. [8], Zhang *et al.* have investigated this kind of shape-invariant rotating beam for the case that $p=l=1,2,3,4$ and $\sigma^2 a=2$ (here σ and a are the parameters in Ref. [8]). But different from our study in this paper, they only considered the evolution of the beam under the condition that the axis of each constituent LG beam is identical to the center of the harmonic potential, and the initial kick on the beam (i.e., $\mathbf{C}_0$) and the initial transverse displacement of the beam from the potential center (i.e., $\mathbf{r}_0$) was not taken into account.

B. Evolution of the rotating pattern

During propagation, the rotating pattern is shape invariant but size variant if the prerequisite in Eq. (26) is satisfied. The pattern shape is closely related to the minimum interval of the topological charges l for the constituent LG beams, represented by Δl. It is Δl that makes the intensity change periodically with the increase of the azimuthal angle $\varphi(z)$. The reason is as follows: For the constituent LG beams with different topological charges, the phases increase along the azimuthal angle with different growth rates. Therefore the constituent beams experience constructive and destructive interference alternatively with the increase of $\varphi(z)$. This leads to a periodical change of the intensity along the azimuthal angle $\varphi(z)$, and the intensity variation period $\Delta\varphi$ is connected with Δl by the relation (as shown in Fig. 2)

$$\Delta\varphi=\frac{2\pi}{\Delta l}. \tag{29}$$

Although the rotating pattern is shape invariant, its size varies periodically during propagation with the period $\Delta z=\pi z_{c0}$, as shown in Eq. (17). Only when the input beamwidth w_0 is exactly equal to w_c (we call it the critical beamwidth) can the beamwidth be kept constant during propagation. Otherwise the beamwidth periodically oscillates about the critical beamwidth (as shown in Fig. 3).

As shown in Eqs. (17) and (24), both the evolution of the rotation angle $\varphi_0(z)$ and that of the beamwidth $w(z)$ are related to the input beamwidth w_0 and the critical beamwidth w_c. Then there may be a question of whether there is a relationship between the two. The answer is yes. In fact, from Eqs. (17) and (24) we have

$$\frac{\partial}{\partial_z}\varphi_0(z)=\frac{1}{w^2(z)}\frac{2p+|l|+\beta}{kl}. \tag{30}$$

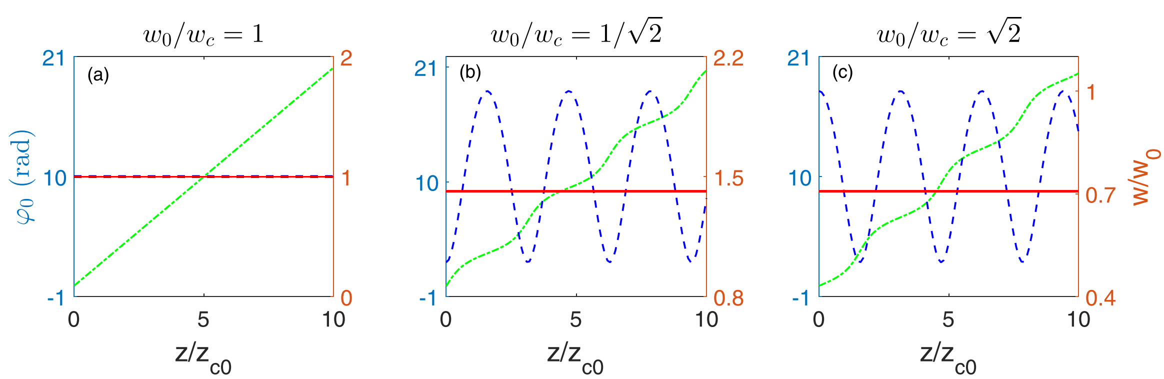

FIG. 3. Evolutions of the beamwidth $w(z)$ (blue dashed line, right ordinate) and the pattern's azimuthal orientation $\varphi_0(z)$ (green dash-dotted line, left ordinate) for different input beamwidths w_0 in the case of $(2p+|l|+1)/l=2$. The red solid line represents the critical beamwidth w_c for comparison.

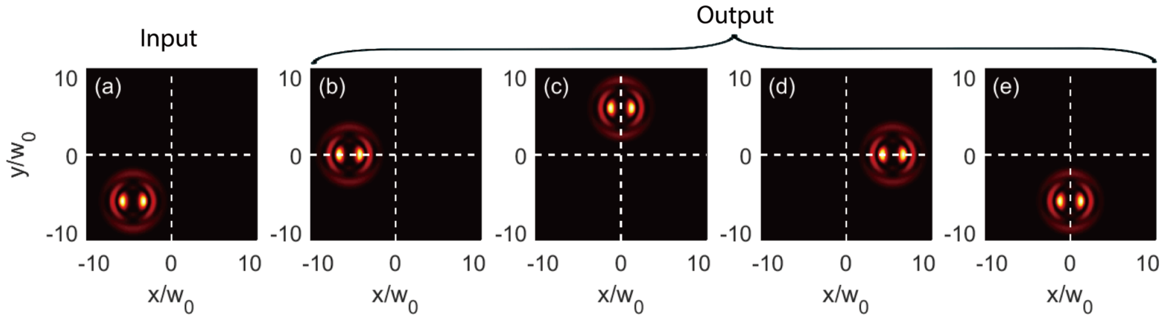

FIG. 4. Different transverse positions of the beam at the exit plane resulting from different initial kicks $\mathbf{C}_0$. (a) The intensity pattern at the entrance plane. (b)–(e) The intensity patterns at the exit plane for ($C_{0x} = -6/w_0$, $C_{0y} = 0$) (b), ($C_{0x} = 0$, $C_{0y} = 6/w_0$) (c), ($C_{0x} = 6/w_0$, $C_{0y} = 0$) (d), and ($C_{0x} = 0$, $C_{0y} = -6/w_0$) (e). The values of the other parameters are $r_{0x} = -5w_0$, $r_{0y} = -6w_0$, $w_0/w_c = 1$, $L = \pi z_{c0}/2$. $\Psi(\mathbf{r}, 0) = 2\Psi_{0,1}(\mathbf{r}, 0) + \Psi_{1,3}(\mathbf{r}, 0) + 0.1\Psi_{2,5}(\mathbf{r}, 0)$.

Obviously, the rotation speed is kept constant only without variation of the beamwidth. Otherwise the rotation speed changes periodically with the period $\Delta z = \pi z_{c0}$, which is equal to that for the variation of the beamwidth. In each period, the larger (smaller) the beamwidth is, the slower (faster) the rotation speed will be (as shown in Fig. 3).

C. Steerable transverse position of the rotating beam at the exit plane

As shown in Eq. (20), during propagation, there is a continuously varied displacement [i.e., $\mathbf{s}(z)$] of the shape-invariant rotating beam from the center of the harmonic potential. In fact, for a medium with a fixed length L, the displacements in the x and y directions at the exit plane can be separately written as

$$s_x(L) = \left[\frac{C_{0x}^2}{k^2} z_{c0}^2 + r_{0x}^2\right]^{1/2} \sin\left[\left(\frac{L}{z_{c0}}\right) + \theta_x\right], \quad (31)$$

$$s_y(L) = \left[\frac{C_{0y}^2}{k^2} z_{c0}^2 + r_{0y}^2\right]^{1/2} \sin\left[\left(\frac{L}{z_{c0}}\right) + \theta_y\right], \quad (32)$$

where

$$\theta_x = \arctan\left(\frac{k r_{0x}}{z_{c0} C_{0x}}\right) + \pi\epsilon(C_{0x}),$$

$$\theta_y = \arctan\left(\frac{k r_{0y}}{z_{c0} C_{0y}}\right) + \pi\epsilon(C_{0y}),$$

$\epsilon(x) = 0$ (for $x \geqslant 0$) or 1 (for $x < 0$). Equations (31) and (32) show that the displacements in the x and y directions at the exit plane can be steered independently. In detail, the displacement in the x direction can be steered by tuning the initial kick C_{0x} and the initial displacement r_{0x} at the entrance plane. The maximum displacement can be obtained as $(C_{0x}^2 z_{c0}^2/k^2 + r_{0x}^2)^{1/2}$. For the case that $(C_{0x}^2 z_{c0}^2/k^2 + r_{0x}^2)^{1/2} = \text{const}$, the magnitude of the displacement in the x direction arrives at its maximum when $L/z_{c0} + \theta_x = (m + 1/2)\pi$ $(m = 0, 1, 2 \ldots)$, and becomes zero when $L/z_{c0} + \theta_x = m\pi$, and so does the displacement in the y direction.

Figure 4 gives an example for the steerable transverse position of the shape-invariant rotating beam at the exit plane. It shows that one can obtain different transverse positions at the exit plane by tuning the initial kicks in the x and y directions, even if the transverse position at the entrance plane is fixed.

Besides, because the initial kick and displacement make the beam sinusoidally oscillate in the x and y directions, the beam undergoes an elliptically spiral trajectory during propagation (as shown in Fig. 1).

IV. CONCLUSION

In conclusion, we have theoretically investigated the propagation dynamics of a type of shape-invariant rotating beam in linear media with an external harmonic potential. By using the technique of variable transformation, we get the analytical solution of the shape-invariant rotating beam, which is constructed by superposing a series of properly selected LG beams with different orders. Based on the analytical solution, we study the propagation properties, which include three aspects: (i) The rotating pattern keeps shape invariant but its size changes periodically. (ii) The pattern rotates either clockwise or anticlockwise around the beam center, depending on the sign of the topological charges of the constituent LG beams, i.e., l. (iii) The transverse position of the beam at the exit plane of a medium can be steered by tuning the input parameters, even if the transverse position at the entrance plane is fixed.

The general formula Eq. (26) can be used as a general method to construct various shape-invariant rotating beams by superposing LG beams of different orders, which may lead to potential applications in particle manipulation. The steerability of the transverse position of the beam at the exit plane might be of interest for signal processing. In addition, because the diffraction of the shape-invariant rotating beam can be balanced by the focusing effect of the harmonic potential, it is possible to construct a rotating linear bullet by combining this type of beam with an Airy pulse in time, which is the only known dispersion-free one-dimensional wave packet.

ACKNOWLEDGMENTS

This research was supported by the National Natural Science Foundation of China (Grants No. 11174090, No. 11174091, and No. 61575068).

[1] Z. Ye, S. Liu, C. Lou, P. Zhang, Y. Hu, D. Song, J. Zhao, and Z. Chen, Acceleration control of Airy beams with optically induced refractive-index gradient, Opt. Lett. **36**, 3230 (2011).

[2] C. Lin, T. Hsiung, and M. Huang, The general potential $V(x,t)$ in which Airy wave packets remain nonspreading, Europhys. Lett. **83**, 30002 (2008).

[3] W. Liu, D. N. Neshev, I. V. Shadrivov, A. E. Miroshnichenko, and Y. S. Kivshar, Plasmonic Airy beam manipulation in linear optical potentials, Opt. Lett. **36**, 1164 (2011).

[4] H. Zhong, Y. Zhang, M. R. Belić, C. Li, F. Wen, Z. Zhang, and Y. Zhang, Controllable circular Airy beams via dynamic linear potential, Opt. Express **24**, 7495 (2016).

[5] C. Hwang, K. Kim, and B. Lee, Dynamic control of circular Airy beams with linear optical potentials, IEEE Photon. J. **4**, 174 (2012).

[6] X. Huang, Z. Deng, and X. Fu, Dynamics of finite energy Airy beams modeled by the fractional Schrödinger equation with a linear potential, J. Opt. Soc. Am. B: Opt. Phys. **34**, 976 (2017).

[7] N. K. Efremidis, Airy trajectory engineering in dynamic linear index potentials, Opt. Lett. **36**, 3006 (2011).

[8] Y. Zhang, X. Liu, M. R. Belić, W. Zhong, F. Wen, and Y. Zhang, Anharmonic propagation of two-dimensional beams carrying orbital angular momentum in a harmonic potential, Opt. Lett. **40**, 3786 (2015).

[9] Y. Zhang, M. R. Belić, L. Zhang, W. Zhong, D. Zhu, R. Wang, and Y. Zhang, Periodic inversion and phase transition of finite energy Airy beams in a medium with parabolic potential, Opt. Express **23**, 10467 (2015).

[10] M. A. Bandres and J. C. Gutiérrez-Vega, Airy-Gauss beams and their transformation by paraxial optical systems, Opt. Express **15**, 16719 (2007).

[11] Z. Pang and D. Deng, Propagation properties and radiation forces of the Airy Gaussian vortex beams in a harmonic potential, Opt. Express **25**, 13635 (2017).

[12] R. Zhao, F. Deng, W. Yu, J. Huang, and D. Deng, Propagation properties of Airy-Gaussian vortex beams through the gradient-index medium, J. Opt. Soc. Am. A **33**, 1025 (2016).

[13] X. Peng, Y. Peng, D. Li, L. Zhang, J. Zhuang, F. Zhao, X. Chen, X. Yang, and D. Deng, Propagation properties of spatiotemporal chirped Airy Gaussian vortex wave packets in a quadratic index medium, Opt. Express **25**, 13527 (2017).

[14] L. Feng, J. Zhang, Z. Pang, L. Wang, T. Zhong, X. Yang, and D. Deng, Propagation properties of the chirped Airy beams through the gradient-index medium, Opt. Commun. **402**, 60 (2017).

[15] J. C. Gutiérrez-Vega and M. A. Bandres, Ince-Gaussian beams in a quadratic-index medium, J. Opt. Soc. Am. A **22**, 306 (2005).

[16] X. Peng, Y. Peng, L. Zhang, D. Li, and D. Deng, Reversed Airy Gaussian and Airy Gaussian vortex light bullets in harmonic potential, Laser Phys. Lett. **14**, 055002 (2017).

[17] V. V. Kotlyar, A. A. Kovalev, and A. G. Nalimov, Propagation of hypergeometric laser beams in a medium with a parabolic refractive index, J. Opt. **15**, 125706 (2013).

[18] M. Newstein and K. Lin, Laguerre-Gaussian periodically focusing beams in a quadratic index medium, IEEE J. Quantum Electron. **23**, 481 (1987).

[19] Y. Zhang, X. Liu, M. R. Belić, W. Zhong, M. Petrovic, and Y. Zhang, Automatic Fourier transform and self-Fourier beams due to parabolic potential, Ann. Phys. **363**, 305 (2015).

[20] Y. Zhang, X. Liu, M. R. Belić, W. Zhong, Y. Zhang, and M. Xiao, Propagation Dynamics of a Light Beam in a Fractional Schrödinger Equation, Phys. Rev. Lett. **115**, 180403 (2015).

[21] N. K. Efremidis, Accelerating beam propagation in refractive-index potentials, Phys. Rev. A **89**, 023841 (2014).

[22] T. Han, H. Chen, C. Qin, W. Li, B. Wang, and P. Lu, Airy pulse shaping using time-dependent power-law potentials, Phys. Rev. A **97**, 063815 (2018).

[23] D. Lu, W. Hu, and Q. Guo, The relation between optical beam propagation in free space and in strongly nonlocal nonlinear media, Europhys. Lett. **86**, 44004 (2009).

[24] A. E. Siegman, *Lasers* (University Science, Mill Valley, CA, 1986).